Nanotechnology **19** (2008) 355707 (7pp) doi:10.1088/0957-4484/19/35/355707

A versatile synthesis of highly bactericidal Myramistin® stabilized silver nanoparticles

G K Vertelov[1], Yu A Krutyakov[1], O V Efremenkova[2], A Yu Olenin[1] and G V Lisichkin[1]

[1] Department of Chemistry, M V Lomonosov Moscow State University, Moscow 119992, Russia
[2] G F Gauze New Antibiotics Research Institute, Moscow 119021, Russia

E-mail: yurii@petrol.chem.msu.ru (Y A Krutyakov)

Received 13 May 2008, in final form 11 June 2008
Published 18 July 2008
Online at stacks.iop.org/Nano/19/355707

Abstract
Silver nanoparticles stabilized by a well-known antibacterial surfactant benzyldimethyl[3-(myristoylamino)propyl]ammonium chloride (Myramistin®) were produced for the first time by borohydride reduction of silver chloride sol in water. Stable aqueous dispersions of silver nanoparticles without evident precipitation for several months could be obtained. *In vitro* bactericidal tests showed that Myramistin® capped silver NPs exhibited notable activity against six different microorganisms—gram-positive and gram-negative bacteria, yeasts and fungi. The activity was up to 20 times higher (against *E. coli*) compared to Myramistin® at the same concentrations and on average 2 times higher if compared with citrate-stabilized NPs.

(Some figures in this article are in colour only in the electronic version)

1. Introduction

It is well known that silver reveals antimicrobial activity [1]. Since the early 1000 BC, silver vessels have been utilized to store potable water [2] and silver compounds—for their medicinal properties—as popular remedies for rheumatism, tetanus, cold, gonorrhea treatment and wound healing long before the age of chemical antibiotics [3, 4]. Now the range for silver applications is only increasing [5]. Silver-containing materials are being utilized to reduce infections in burn treatment and arthroplasty, to prevent bacteria growth on prostheses, catheters, dental materials, vascular grafts, stainless steel materials, on textile fabrics and so on [6].

In medical applications silver in the form of nanoparticles (NPs) is a promising alternative to silver salts and bulk metal because salts may possess quick and uncontrolled silver release while bulk metal is a too slow and inefficient releasing system. Thus, it should be mentioned that the NPs exhibit different physical properties from those of ions and bulk metals. NPs represent a great combination of small size (1/1000 of a bacterium) and at the same time a large number of atoms—more than 1000 in one 5 nm particle. In that way, silver NPs have been broadly studied for their antimicrobial activity [7–10]. The activity is comparable to that of a broad spectrum of the most prominent antibiotics used worldwide [11]. One also should take into account the relative innocence of silver sols (in comparison with most strong antibiotics) and a unique advantage that bacteria do not mutate to diminish silver effectiveness [12].

It is still not clear the mechanism of silver antimicrobial action. It has been proposed that silver ions can interact with thiol groups of some vital protein or enzyme, deactivating them [13, 14]. The other targets can be chloride ions, RNA or DNA. Experimental data shows that DNA bound with silver loses its replication ability [15]. NPs being introduced into a bacteria-containing medium may act as a constant origin of metal ions upon the particles' slow oxidation. Moreover, silver NPs with sizes up to 10–20 nm are accumulated within living cells, thereby demonstrating an active transport throughout the membrane [9, 16] and working as a special biocidal agent (in the case of *P. aeruginosa* the authors found that even 80 nm particles can transport through the inner and outer cellular membrane [17]). When silver sols are used along with traditional antibiotics there is some evidence of a synergetic effect with increase in efficacy up to tenfold [18, 19]. Silver NPs capped with norvancomycin caused a growth delay of *E. coli*, while vancomycin itself had no significant influence

on the bacterial evolution [20]. In explanation of this the membrane transport of nanoparticles can also play a key role.

Although norvancomycin-capped silver nanoparticles exhibited promising results it is still required to obtain silver particles first and modify them second, not mentioning the purification. To our thinking it would be much easier from the synthetic point of view when an antibiotic is, at the same time, a stabilizer for nanoparticles and a surfactant. The best candidate for that in our opinion was benzyldimethyl[3-(myristoylamino)propyl]ammonium chloride monohydrate, known as Myramistin®—an antiseptic with a wide range of action, which is being used for tropical disinfection and healing of wounds, scratches, tropical ulcers, herpes, stomatitis, angina and venereal diseases [21, 22]. The compound is active against a large group of gram-positive and gram-negative bacteria and is a typical surfactant. The typical range of therapeutic concentrations for Myramistin® is 0.01–2 wt% [21, 22]: the high content of it could be a reason why Myramistin® as a drug has some restrictions for its applications. In the present investigation, we for the first time report on obtaining silver NPs stabilized with Myramistin® and studying their antimicrobial activity.

2. Experimental procedure

2.1. Chemicals

Benzyldimethyl[3-(myristoylamino)propyl]ammonium chloride monohydrate (0.01% solution in water) was purchased from Infamed (Russia) and used without any modifications. Silver nitrate (99.9+%, Sigma-Aldrich), sodium citrate dihydrate (99+%, Sigma-Aldrich) and sodium borohydride (Lancaster, 98+%) were of analytical grade and used without further purification. All aqueous solutions were prepared with doubly distilled water.

2.2. Synthesis of Myramistin® stabilized silver NPs

The preparation of Myramistin® stabilized Ag NPs was performed as follows. Ten milliliters of $AgNO_3$ (0.02 g, 1.18×10^{-4} mol) water solution was added dropwise to 100 ml of 0.01% Myramistin® aqueous solution with vigorous stirring. The mixture was kept stirred for 15 min, and after that 90 ml of $NaBH_4$ (0.01 g, 2.6×10^{-4} mol) and Myramistin® (0.01 g, 2.25×10^{-5} mol) combined water solution was added dropwise with intense stirring. The quantity of silver nitrate added was adjusted to reach 10^{-4} g ml^{-1} total concentration of silver in the reaction mixture. The quantity of Myramistin® was adjusted to 10^{-4} g ml^{-1} total concentration in the reaction mixture. After complete addition of sodium borohydride the mixture was stirred for 1 h.

2.3. Synthesis of citrate-stabilized silver NPs

Briefly, 50 ml of $AgNO_3$ (0.0063 g, 3.7×10^{-5} mol) aqueous solution was added dropwise to 50 ml sodium citrate solution with vigorous stirring. Then 100 ml of $NaBH_4$ (0.003 g, 8×10^{-5} mol) was added dropwise with intense stirring. The quantity of sodium citrate added was adjusted to reach 3×10^{-4} mol l^{-1} total concentration of citrate in the reaction mixture according to [23].

2.4. Measurements

The UV–vis absorbance spectra were recorded using a Jenway 6310 spectrophotometer (Bibby Scientific Ltd), and 10 mm path length quartz cuvettes were used for measurement of solution spectra.

The electronic images and diffractograms were made on a Leo 912 AB Omega (Leo Ltd) transmission electron microscope (TEM) operating at 100 kV. The samples for TEM characterization were prepared by placing a drop of a colloidal solution on a formvar-coated copper grid which was dried at room temperature. All size distributions were calculated using Femtoscan Online v. 2.2.91 software (Advanced Technologies Center, Russia).

X-ray photoelectron spectra were taken in a LAS-3000 spectrometer (Riber, France) with ESCA hemispherical electron analyzer OPX-150. The apparatus was equipped with a monochromatic Al Kα source of x-ray radiation (1486.6 eV). The base pressure of the spectrometer was in the 10^{-10} Torr range. The binding energies were corrected for a specimen charging by referencing the C 1s peak to 284.6 eV. The XPS analyses were performed by assuming core-level spectra with Gaussian lineshapes after standard Shirley background subtraction. Samples were prepared by dispersion on an aluminum sample holder prior to each experiment.

Dynamic light scattering and zeta potential measurements of the obtained dispersions were carried out on a Zetasizer Nano ZS analyzer with integrated 4 mW He–Ne laser, $\lambda = 633$ nm (Malvern Instruments Ltd). Zeta potential was measured by applying an electric field across the dispersion of silver NPs using the technique of laser Doppler anemometry.

2.5. Bactericidal tests

All glassware used was sterilized under high temperature; operations were performed on a cleaned workbench. Antimicrobial activities of the synthesized silver colloids were performed using the standard dilution micromethod, determining the minimum inhibitory concentration (MIC) leading to inhibition of bacterial growth.

Bacterial growth was studied in a liquid nutrition media, as well as on agar plates. Submerged tests were done in a water bath shaker (200 rpm, temperature control). Liquid #2 Gause (G) medium was prepared by dissolving 10 g glucose, 5 g peptone, 3 g tryptone and 5 g NaCl in 1 l of distilled water and subsequent sterilization of the medium at high temperature and pH of the medium was 7.2–7.4. Solid #2 Gause (G) medium was obtained by adding 20 g of agar to the liquid media, heating the mixture and pouring into glass culture dishes.

The following bacterial strains were used to study antimicrobial activities: *Staphylococcus aureus* FDA 209P (MSSA, with meticillin resistance 0.125 mcg ml^{-1}), *S. aureus* INA 00761 (MRSA, with meticillin resistance 32 mcg ml^{-1}), *Leuconostoc mesenteroides* VKPM B-4177 (with vancomycin resistance more than 512 mcg ml^{-1}), *Escherichia coli* ATCC

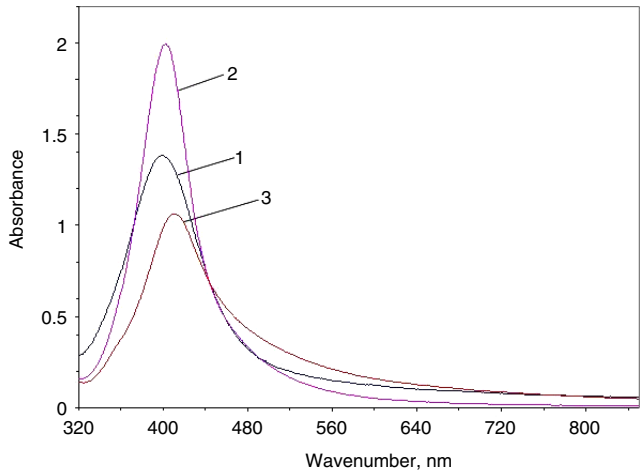

Figure 1. UV–vis absorbance spectra of aqueous dispersions of silver NPs capping with: (1)—citrate; (2)—Myramistin®; (3)—Myramistin® (aged 2 months).

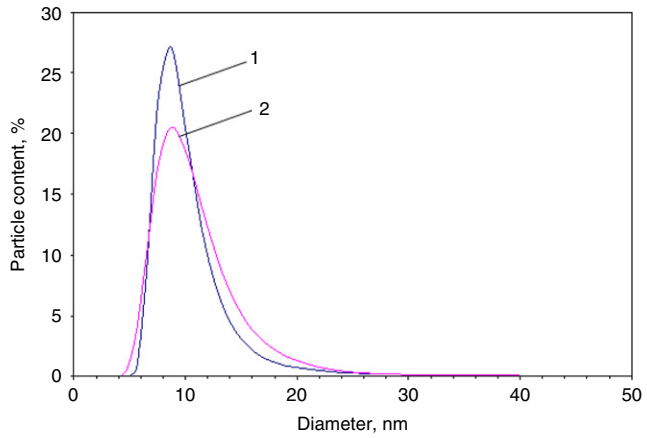

Figure 2. DLS data on particle size distribution of (1) citrate-stabilized Ag NPs and (2) Myramistin® stabilized Ag NPs.

25922, *Aspergillus niger* INA 00760 and *Saccharomyces cerevisiae* RIA 259.

The silver NPs solutions were added to the nutrition media to have 2–128 times dilution of silver NPs in the media. In the case of agar media NP solutions were added while the agar medium was still hot (for better distribution of the particles and to sterilize the solutions of NPs). The minimal inhibition concentrations (MICs) were read after 24 h of incubation at 37 °C (strains FDA 209P, INA 00761, ATCC 25922) and 28 °C (strains VKPM B-4177, INA 00760, RIA 259) as the MICs of tested silver NPs that inhibited the bacterial growth.

To determine the MIC in a liquid medium, 10^7 colony forming units (cfu ml^{-1}) of a bacterial strain were grown in 1 ml of the liquid G medium supplemented with tested silver NPs. Sets were incubated in the shaker. To study the bacterial growth on agar plates 50 mcL 10^7 cfu ml^{-1} suspension of a bacterium were evenly distributed on the agar G medium surface supplemented with tested silver NPs.

Cultural growth was at 37 °C (strains FDA 209P, INA 00761, ATCC 25922) and 28 °C (strains VKPM B-4177, INA 00760, RIA 259) about 17–24 h.

3. Results and discussion

3.1. Formation of the silver NPs

To determine the optimum conditions for the synthesis of stable Myramistin® stabilized NPs with narrow size distribution several experiments were carried out varying the concentration of reagents and the order of their addition to the reaction mixture. It has been found that an optimal order consisted in initial dropwise addition of silver salt solution to Myramistin® to obtain a stable sol of AgCl. Myramistin® is a typical cationic surfactant with a molecular structure shown below.

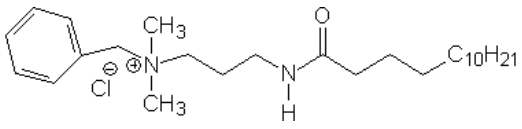

The second step was reducing silver chloride NPs to silver NPs. The manner of preparation of citrate-stabilized silver NPs was found to be the same and the optimal concentration of citrate anion turned out to be in good agreement with [23]. Electronic spectra of aqueous dispersions of the metal are presented in figure 1.

They exhibited surface plasmon bands at 400–413 nm corresponding to non-covalently stabilized Ag NPs. In contrast to gold [24], there is no good correlation between the size distribution of silver NPs and the position of their SPR peak. However, the peak maximum after two months of aging shifted to a red region (413 nm against 405 nm for freshly prepared NPs). Though it is difficult to estimate particle size and aggregation behavior of silver NPs analyzing peak bandwidth, it may be concluded that after two months of aging Ag NPs have a larger mean diameter and broader size distribution in comparison with freshly prepared NPs.

3.2. DLS and TEM study

To monitor the size distribution of prepared NPs we applied a method of dynamic light scattering (DLS). Unlike TEM, this method allows us to estimate size distribution and aggregation behavior of sols under real conditions. Figure 2 demonstrates size distributions of citrate and freshly prepared Myramistin® stabilized Ag NPs.

As can be seen the mean diameters for the NPs were around 9–10 nm for citrate-stabilized NPs and 10 nm for Myramistin® stabilized.

On the other hand, Myramistin® stabilized Ag NPs after two months of aging have revealed a greater mean diameter (51 nm) and broader size distribution upon DLS investigation (see figure 3).

It is no doubt that Myramistin® stabilized silver NPs continue to undergo dissolving and growing, and aggregation processes while staying at room temperature. To estimate the stability to aggregation of the obtained systems the zeta potential (zeta) for the NP sols was evaluated. In general, the zeta potential absolute value can be utilized as an indicator of the stability of a colloidal system. The higher the zeta

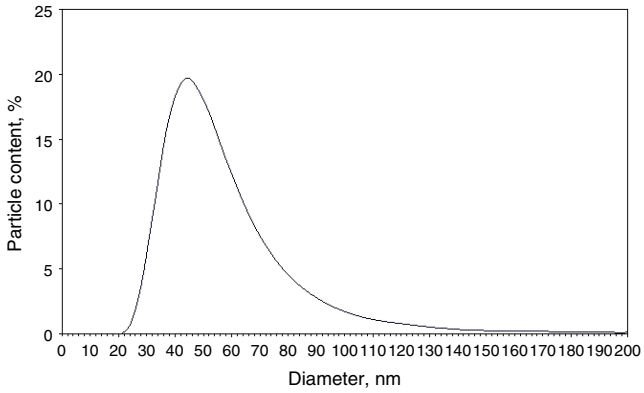

Figure 3. DLS data on particle size distribution of Myramistin® stabilized Ag NPs aged 2 months.

Table 1. Zeta potential measurements and average diameter data of synthesized silver NPs.

	NanoAg-citrate	NanoAg-Myramistin®	NanoAg-Myramistin® aged
Zeta (mV)	-29.1 ± 0.5	$+31.0 \pm 1.6$	35.0 ± 0.8
pH	7.8	8.8	8.2
d (nm)	9.0 ± 0.9	10.0 ± 1.8	51 ± 6

absolute values, the higher the potential difference between the dispersion medium and the slipping plane, hence the charge onto the surface of the particles and, therefore, the larger the electrostatic repulsion between particles[3]. The value of 25 mV is referred to as a boundary value separating low and highly charged surfaces; the theoretical limit of stability is |30| mV, i.e. a colloidal system will be stable if its zeta potential is higher than 30 mV or lower than −30 mV [25]. Both Myramistin® and citrate-stabilized silver NPs were found to have zeta absolute values around 30 mV (see table 1), which is, according to [26], the boundary state between incipient instability and moderate stability.

The signs of the zeta potentials correlate with the charge signs of surfactants—'negative' for citrate and 'positive' for Myramistin®.

The DLS data are in good agreement with TEM studies. Typical TEM pictures, electron diffraction (ED) patterns and size distribution histograms are presented in figures 4–6. From electron microdiffraction all of the colloidal particles can be classified as crystalline. Only the diffraction rings of silver are found in each ED pattern.

Figures 4–6 illustrate the size distribution and typical shapes of the obtained silver nanoparticles. Citrate-stabilized NPs exhibited almost a bimodal size distribution, with two maxima at 2 and 14 nm and an average diameter of 9 nm; as for freshly prepared NanoAg-Myr—8.5 nm. The aged NanoAg-Myr not only has larger particles, but also many aggregated patterns. In spite of the NPs aggregation, there were no indications of bulk silver precipitation in the silver sols.

[3] Fe_2O_3.

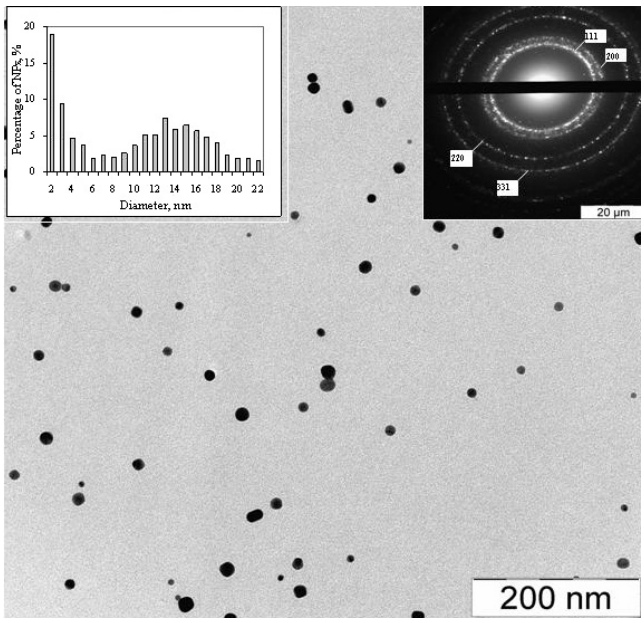

Figure 4. TEM image, electron microdiffraction and particle size distribution of citrate-stabilized silver NPs.

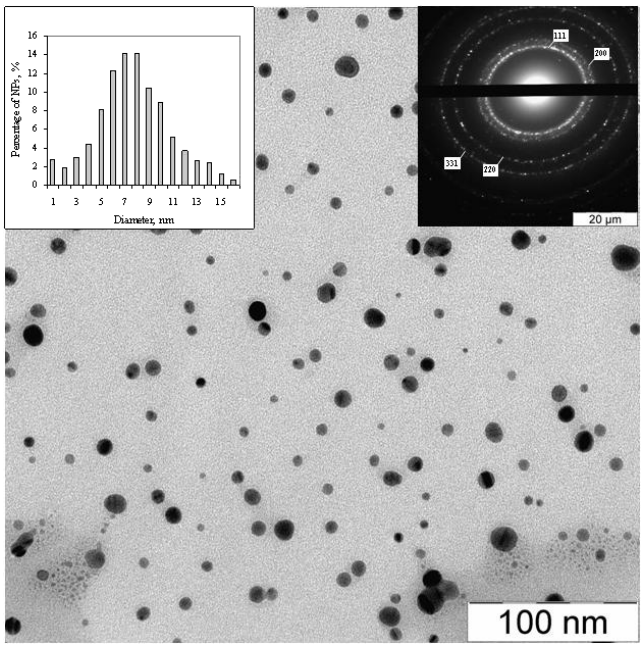

Figure 5. TEM image, electron microdiffraction and particle size distribution of freshly prepared Myramistin® stabilized silver NPs.

Finally clear evidence of Myramistin® attachment to the surface of the NPs was also provided by XPS spectroscopy of dry samples.

3.3. XPS characterization

X-ray photoelectron spectra provide information about binding energies of inner shell electrons of Ag and the stabilizer's molecules on the surface of NPs. The main peaks observed

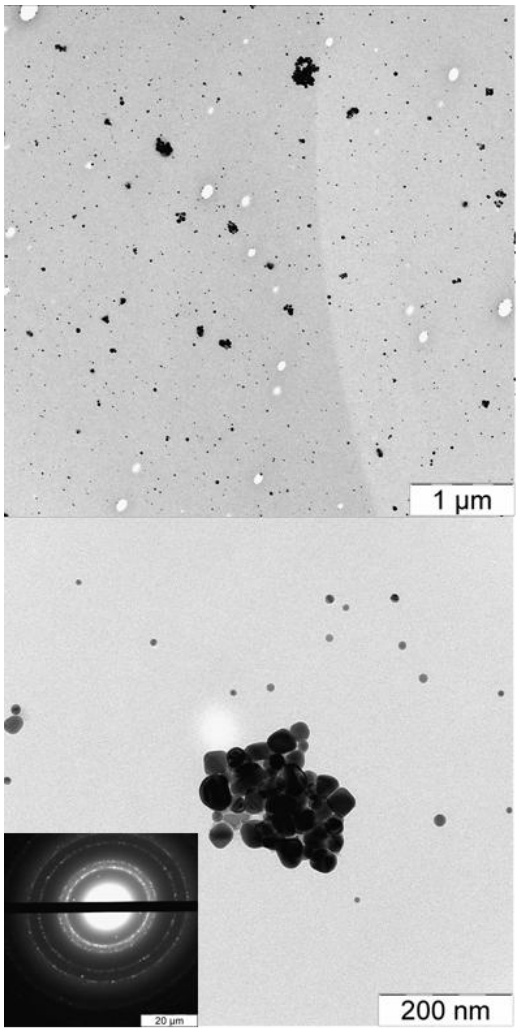

Figure 6. TEM images and electron microdiffraction of Myramistin® stabilized silver NPs after 2 months of aging.

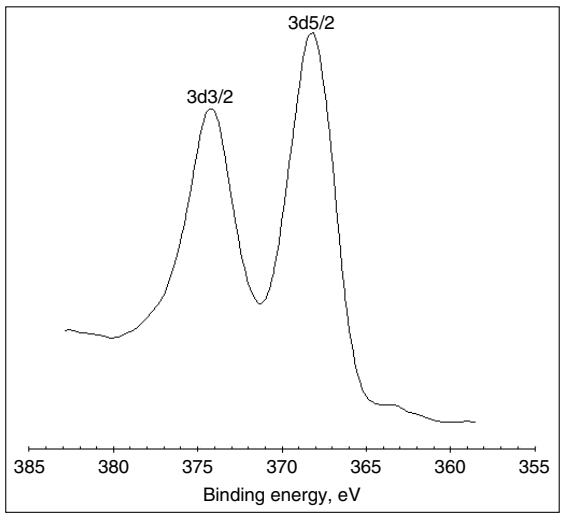

Figure 7. Ag 3d XPS spectrum of silver NPs prepared by borohydride reduction of AgCl aqua sols in the presence of Myramistin®.

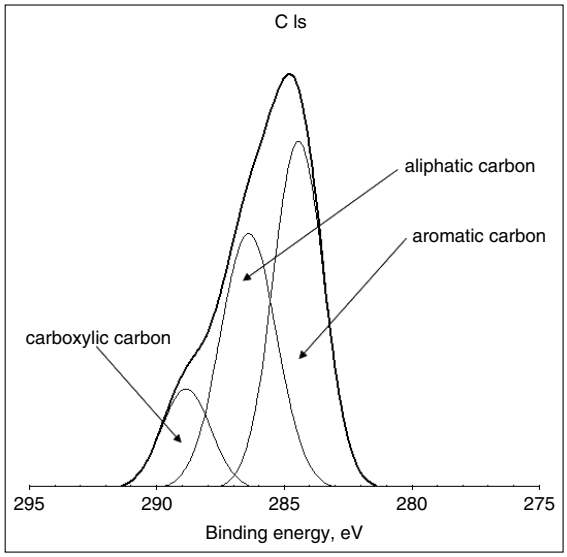

Figure 8. C 1s XPS spectrum of silver NPs prepared by borohydride reduction of AgCl aqua sols in the presence of Myramistin®.

in the survey scan (not shown) of the sample are C1s$_{1/2}$, N 1s$_{1/2}$, O 1s$_{1/2}$, Ag 3s, Ag 3p, Ag 4p and Ag 4d peaks. The binding energies (BE) of Ag 3d$_{5/2}$ and Ag 3d$_{3/2}$ for silver NPs are shown in figure 7.

The Ag 3d spectrum exhibits peaks at 368.3 eV (3d$_{5/2}$) and 374.0 eV (3d$_{3/2}$), which correspond to that of silver in the zero valence state [27].

It is clear that Myramistin® contains carbon in a different oxidation state, namely carbon from carboxyl, aliphatic and aromatic groups. Figure 8 shows the C 1s core-level spectra for Myramistin® stabilized Ag NPs.

In order to obtain more detailed knowledge about surface chemistry the C 1s spectrum for the Myramistin® stabilized silver NPs has been resolved by superposition of three peaks corresponding to various carbon atoms of Myramistin®. The different environments for carbon on the NP surface are clear evidence of the presence of a stabilizer. The higher BE peak should be associated with aromatic carbon environments present in the sample. This value is in good agreement with the BE position for C 1s core level found by [28]. The lower BE peak should be attributed to carboxylic groups of Myramistin® molecules [28]. The medium peak in the spectrum corresponds to aliphatic carbon [28]. The N 1s$_{1/2}$ region in figure 9 is, unfortunately, overlapping with the signal of a silver satellite peak, thus hindering a good correlation for the signals in the region, although we can guess about the presence of signals corresponded to tertiary and amide nitrogen in the region 399–403 eV.

An unavoidable superposition of Ag 3d (satellite) and N 1s peaks does not allow us to discriminate correctly the contribution of peaks corresponding to tertiary and amide nitrogen in the total signal.

4. Antimicrobial study

The standard dilution micromethod was applied in performing the antimicrobial activity tests in liquid #2 G medium and on

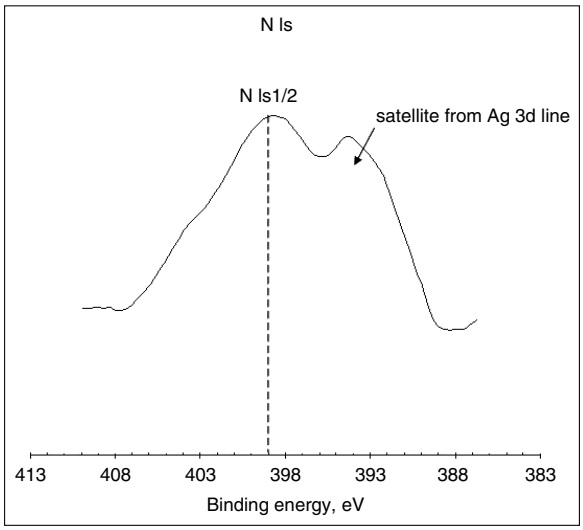

Figure 9. N 1s XPS spectrum of silver NPs prepared by borohydride reduction of AgCl aqua sols in the presence of Myramistin®.

Table 2. MICs of tested samples for *Escherichia coli* ATCC 25922 *(E. coli)* and *Staphylococcus aureus* FDA 209P *(St. 209)* strains.

	MIC (mcg ml^{-1})			
	Liquid media		Agar plates	
	E. coli	*St. 209*	*E. coli*	*St. 209*
Myramistin®	>20	20	>10	5
Na citrate	—	—	—	—
Ag+	<10	5	<5	>5
NanoAg-Myr	<1	5	2.5	2.5
NanoAg-Cit	10	5	5	5

the agar plates, supplemented with tested silver NPs. Silver NPs, both citrate and Myramistin® stabilized, were subjected to antimicrobial tests. The dilutions used of NPs ranged from 2 up to 128 times. Firstly only two types of bacteria were exploited—gram-negative *Escherichia coli* ATCC 25922 and gram-positive *Staphylococcus aureus* FDA 209P. Minimal inhibition concentrations (MICs) of the tested samples are summarized in table 2.

As seen from the table MIC of controlling samples containing only Myramistin® and silver ions are higher in comparison with NPs capped with Myramistin®. Moreover MICs for citrate-stabilized NPs (NanoAg-Cit) are close in values to MICs for silver cations, which is not surprising since the antimicrobial activity of NanoAg-Cit can be mostly due to silver ion diffusion from NPs (samples containing sodium citrate have not shown any inhibition of bacterial growth in the concentration range studied).

There is no specific mechanism of silver NP action against different types of bacteria (except for the necessity to penetrate throughout the additional membrane in the case of gram-negative bacteria); hence antibiotic-resistant and nonresistant bacteria are equivalent targets for the NPs, which is an advantage of NP-based antibiotic substances when a broad spectrum and gentle action are needed. Extending the number of studied bacteria we showed that NanoAg-Myr particles are equally effective against highly meticillin-resistant *Staphylococcus aureus* INA 00761 and vancomycin-resistant *Leuconostoc mesenteroides* VKPM B-4177; fungi *Aspergillus niger* INA 00760 and yeasts *Saccharomyces cerevisiae* RIA 259. Myramistin® itself revealed up to fourfold less activity, while citrate-stabilized silver sols showed comparable bactericidal activity, having two times lower MIC against *Staphylococcus aureus* INA 00761 (see table 3).

Table 3. MICs of tested samples for *Staphylococcus aureus* INA 00761 *(St. A)*, *Leuconostoc mesenteroides* VKPM B-4177 (*Leu.*), *Saccharomyces cerevisiae* RIA 259 (*Sacc.*) and *Aspergillus niger* INA 00760 *(Asp.)* strains.

	MIC (mcg ml^{-1})			
	St. A	*Leu.*	*Sacc.*	*Asp.*
Myramistin®	10	10	>20	>20
Na citrate	—	—	—	—
NanoAg-Myr	2.5	5	5	5
NanoAg-Cit	5	5	5	5

Myramistin® acting as a surfactant interacts with the cell membrane, diminishing its stability and increasing permeability. Silver NPs are also considered to act that way [20]. Combing two substances in one—Myramistin® stabilized silver NPs—brings about a reinforcing of antibiotic activity. We speculate that upon the approach of NanoAg-Myr NPs to a cell wall Myramistin® of the particles or Myramistin® of the surrounding medium interacts with the wall, weakening it and allowing the NPs to penetrate through the membrane faster and easier. Thus it could be explained why NanoAg-Myr has ten times lower MIC against *E. coli* compared to NanoAg-Cit and 20 times lower compared to Myramistin® (table 2)—-it is the synergetic action of both Myramistin® and silver NPs.

It has to be mentioned that Myramistin® stabilized silver NPs which were aged for two months exhibited unexpectedly high antibiotic activity. Some preliminary studies showed the MICs against *E. coli* and *S. aureus*. The noted NPs decreased to 0.3 and 0.1 mcg ml^{-1}, respectively, that is ten times lower than for freshly prepared NAg-Myr and 100 times lower than for Myramistin® itself. These promising results are not easy to interpret. On the one hand, there are several studies that showed a strong correlation between antibiotic activity of silver NPs and their size distribution—the smaller, the more active [9]. On the other hand, larger particles contain more Myramistin® on their surface. It is also to be said that small silver NPs (smaller than 10 nm) due to their ability to penetrate through almost any membrane, irrespective of its nature—host or bacteria cells, are considered to have some hazardous impact on host cells too [29]. Thus, high antibiotic activity of the aged NAg-Myr, containing large aggregates of silver NPs, seems to us favorable for its future applications.

5. Conclusions

The silver nanoparticles stabilized with Myramistin®, a commercially available antimicrobial agent, were synthesized for the first time in this report. The formation of the NP sols was first verified with UV–vis absorption spectra. The

size distribution was found out by DLS and TEM analyses, followed by XPS for more detailed chemical analysis. *In vitro* bactericidal tests showed that Myramistin® capped silver NPs exhibited notable activity against six different microorganisms—gram-positive and negative bacteria, yeasts and fungi. The activity was greater, up to 20 times (against *E. coli*), compared to Myramistin® of the same concentrations and on average 2 times higher if compared with citrate-stabilized NPs. The antibacterial effect was independent of any acquisition of resistance by the bacteria against antibiotics. We speculated on the major mechanism of the NAg-Myr action to be as follows. Myramistin® from the particles or surrounding media anchors to the cell wall, weakening it for the subsequent penetration of silver NPs inside the cell. Aged NAg-Myr appeared to be almost 10 times more active against *S. aureus* and *E. coli*. There is no clear evidence for reliable interpretation of the results. But the key factors could be: change in NP size and compacting of the NP stabilizing Myramistin® layer, thus increasing Myramistin® local surface concentration. Having in mind the potential hazardous impact of very small silver NPs, high bactericidal activity of the largely aggregated aged NanoAg-Myr particles is very favorable for its possible future antimicrobial application. However, further studies must be conducted to study the mechanism of NanoAg-Myr action and the influence of size distribution of the particles on their antimicrobial activity. Certainly, it has to be verified if the bacteria develop resistance towards the NPs and to examine the cytotoxicity of the NPs towards human cells, though it is clear now that the NanoAg-Myr system represents an advantageous model for the future development of a new effective antimicrobial agent with a broad spectrum of action.

References

[1] Klasen H J 2001 Historical review of the use of silver in the treatment of burns. I. early uses *Burns* **26** 117–30

[2] Russell A D and Hugo W B 1994 Antimicrobial activity and action of silver *Prog. Med. Chem.* **31** 351

[3] Mirsattari S M, Hammond R R, Sharpe M D, Leung F and Young G B 2004 Myoclonic status epilepticus following repeated oral ingestion of colloidal silver *Neurology* **62** 1408–10

[4] Atiyeh B S, Costagliola M, Hayek S N and Dibo S A 2007 Effect of silver on burn wound infection control and healing: review of the literature *Burns* **33** 139–48

[5] Krutyakov Yu A, Kudrinskiy A A, Olenin A Yu and Lisichkin G V 2008 Synthesis and properties of silver nanoparticles: achievements and prospects *Russ. Chem. Rev.* **77** 233–57

[6] Silver S 2003 Bacterial silver resistance: molecular biology and uses and misuses of silver compounds *FEMS Microbiol. Rev.* **27** 341–53

[7] Silver S, Phung L T and Silver G 2006 Silver as biocides in burn and wound dressings and bacterial resistance to silver compounds *J. Ind. Microbiol. Biotechnol.* **33** 627–34

[8] Clement J L and Jarrett P S 1994 Antibacterial silver *Met. Based Drugs* **1** 467–82

[9] Morones J R, Elecheguerra J L, Camacho A, Holt K, Kouri J B, Ramirez J T and Yacaman M J 2005 The bactericidal effect of silver nanoparticles *Nanotechnology* **16** 2346–53

[10] Sondi I and Salopek-Sondi B 2004 Silver nanoparticles as antimicrobial agent: a case study of *E.Coli* as a model for gram-negative bacteria *J. Colloid Interface Sci.* **275** 177–82

[11] Revelli D A, Wall D and Leavit R W 2000 Antimicrobial activity of American silver's ASAP solution *Report* American Biotech Labs Alpine, UT

[12] Roy R, Hoover M R, Bhalla A S, Slaweckl T, Dey S, Cao W, Li J and Bhaskar S 2007 Ultradilute Ag-aquasols with extraordinary bactericidal properties: role of the system Ag–O–H_2O *Mater. Res. Innov.* **11** 3–18

[13] Gupta A, Maynes M and Silver S 1998 Effects of halides on plasmid-mediated silver resistance in *Escherichia coli Appl. Environ. Microbiol.* **64** 5042–5

[14] Matsumura Y, Yoshikata K, Kunisaki S and Tsuchido T 2003 Mode of bactericidal action of silver zeolite and its comparison with that of silver nitrate *Appl. Environ. Microbiol.* **69** 4278–81

[15] Feng Q L, Wu J, Chen G Q, Cui F Z, Kim T N and Kim J O 2000 A mechanistic study of the antibacterial effect of silver ions on *Escherichia coli* and Staphylococcus aureus *J. Biomed. Mater. Res.* **52** 662–8

[16] Raffi M, Hussain F, Bhatti T M, Akhter J I, Hameed A and Hasan M M 2008 Antibacterial characterization of silver nanoparticles against *E. Coli* ATCC-15224 *J. Mater. Sci. Technol.* **24** 192–6

[17] Xu X-H N, Brownlow W J, Kyriacou S V, Wan Q and Viols J J 2004 Real-time probing of membrane transport in living microbial cells using single nanoparticles optics and living cell imaging *Biochemistry-US* **43** 10400–13

[18] Souza A de, Mehta D and Leavitt R W 2006 Bactericidal activity of combinations of Silver–Water Dispersion™ with 19 antibiotics against seven microbial strains *Curr. Sci.* **91** 926–9

[19] Li P, Wu C, Wu Q and Li J 2005 Synergetic antibacterial effects of b-lactam antibiotic combined with silver nanoparticles *Nanotechnology* **16** 1912–7

[20] Wei Q S, Ji J, Fu J H and Chen J C 2007 Norvancomycin-capped silver nanoparticles: synthesis and antibacterial activities against *E. coli Sci. China* B **50** 418–24

[21] Cook E V and Moss P H 1949 Quaternary ammonium compounds *US Patent Specification* 2 459 062 Jan. 11

[22] Krivoshein Yu S, Rudko A P and Pavlyuk V G PCT/RU92/00138, publ. No WO93/00892, Jan. 21, 1993

[23] Henglein A and Giersig M 1999 Formation of colloidal silver nanoparticles: capping action of citrate *J. Phys. Chem.* B **103** 9533–9

[24] Khlebtsov B, Zharov V, Melnikov A, Tuchin V and Khlebtsov N 2006 Optical amplification of photothermal therapy with gold nanoparticles and nanoclusters *Nanotechnology* **17** 5167–79

[25] Malvern Instruments 2004 *Hardware Manual: Zetasizer Nano Series* Manual # MAN 0317. Issue 1.1. United Kingdom Malvern

[26] Zeta Potential of Colloids in Water and Waste Water 1985 *ASTM Standard D 4187-82* American Society for Testing and Materials

[27] Kumar A, Joshi H, Pasricha R, Mandale A B and Sastry M 2003 Phase transfer of silver nanoparticles from aqueous to organic solutions using fatty amine molecules *J. Colloid Interface Sci.* **264** 396–401

[28] Beamson G and Briggs D 1992 *High Resolution XPS of Organic Polymers: The Scienta ESCA300 Database* (New York: Wiley)

[29] Oberdorster G, Stone V and Donaldson K 2007 Toxicology of nanoparticles: a historical perspective *Nanotoxicology* **1** 2–25